

Synthesis and electrochemical properties of *p*-cymene-ruthenium(II) complexes with (EPh₂)₂CHR (E = S, Se; R = H, Me) and their anionic derivatives as ligands. Crystal structure of [(η⁶-MeC₆H₄Prⁱ)Ru{η³-(SPh₂)₂CMe-C,S,S'}]PF₆

Mauricio Valderrama*, Raúl Contreras, Verónica Arancibia, Patricio Muñoz

Departamento de Química Inorgánica, Facultad de Química, Pontificia Universidad Católica de Chile, Casilla 306, Santiago-22, Chile

Received 7 November 1995

Abstract

The synthesis and properties of cationic complexes of general formula [(η⁶-MeC₆H₄Prⁱ)RuCl{η²-(EPh₂)₂CHR-E,E'}]BF₄ (R = H, E = S (1), Se (2); R = Me, E = S (5)) are described. The methylene proton of the coordinated dichalcogenide ligand reacts with strong bases such as KOH in methanol or TIPz in dichloromethane solutions, to give new cationic complexes in which the anionic ligand is acting as tridentate chelate with a C,E,E'-donor set, [(η⁶-MeC₆H₄Prⁱ)Ru{η³-(EPh₂)₂CR-C,E,E'}]A (R = H, A = BF₄⁻, E = S (3), Se (4); R = Me, A = PF₆⁻, E = S (6)). The complexes have been characterised by elemental analyses, molar conductivities and IR and NMR spectroscopy. The structure of the title complex was established by X-ray crystallography. The crystals are tetragonal; at 293°C *a* = 15.120(2), *c* = 16.090(3) Å, space group *P*4₃, *Z* = 4. The complex contains a tridentate C,S,S'-bonded ligand occupying three coordination positions of a distorted octahedral ruthenium centre, with an η⁶-MeC₆H₄Prⁱ group completing the coordination sphere. Cyclic voltammetry shows that under argon the acidic protons of the coordinated neutral disulfide ligands (1, 5) are reduced to hydrogen yielding the complexes with the anionic ligand coordinated in their tridentate form (3, 6). These compounds are irreversibly reduced in a one-electron process to give Ru(I) species, followed by chemical decomposition.

Keywords: Ruthenium(II) complexes; Dichalcogenide complexes; Arene complexes; Electrochemistry; Crystal structures

1. Introduction

Recent studies have shown that the methylene protons of coordinated bis(diphenylphosphino)methane disulfide or diselenide ligands in organotransition metal complexes, can be easily removed by bases to give complexes with the anionic methyne form acting as an E,E'- or C,E-bonded chelate ligand [1–5]. In this context, we have recently reported the deprotonation reactions on the coordinated ligands of complexes of the type [(ring)MCl(η²-L)]⁺, where (ring)M = (η⁵-C₅Me₅)Rh, (η⁵-C₅Me₅)Ir, (η⁶-C₆Me₆)Ru and L = (SPh₂)₂CH₂ or (SePh₂)₂CH₂, obtaining new cationic complexes of formula [(ring)M(η³-L')]⁺ in which the resulting anionic ligands are bound to the metal centre as a C,E,E'-tridentate ligand [6–9].

In this paper we report the synthesis of new *p*-cymene-ruthenium(II) cationic complexes with the symmetrical dichalcogenide ligands (SPh₂)₂CH₂, (SePh₂)₂CH₂ and

(SPh₂)₂CHMe, and their methanide anions. The structure of the complex [(η⁶-MeC₆H₄Prⁱ)Ru{η³-(SPh₂)₂CMe-C,S,S'}]PF₆, determined by single crystal X-ray diffraction, is also reported. The electrochemical properties of the disulfide complexes have been studied by cyclic voltammetry in acetonitrile solution.

2. Experimental

2.1. Physical measurements

Elemental analyses were made with Heraeus Mikro Standard and Perkin-Elmer 240B microanalysers. IR spectra were recorded on a Bruker IFS-25 spectrophotometer (over the range 4000–400 cm⁻¹) using KBr pellets. Conductivities were measured in ~5 × 10⁻⁴ M acetone solution using a WTW LF-521 conductimeter. ¹H (200.13 MHz), ³¹P{¹H} (81.01 MHz) and ¹³C{¹H} (50.32 MHz) NMR spectra were

* Corresponding author.

recorded on a Bruker AC-200P spectrometer and chemical shifts are reported relative to SiMe₄ and 85% H₃PO₄ in D₂O (positive shifts downfield).

All reactions were carried out by Schlenk techniques under purified nitrogen. Reagent grade solvents were dried, distilled, and stored under a nitrogen atmosphere. The ligands (SPPPh₂)₂CH₂, (SePPh₂)₂CH₂, (SPPPh₂)₂CHMe and the starting binuclear complex [((η⁶-MeC₆H₄Prⁱ)RuCl(μ-Cl))₂] were prepared by published procedures [10–12].

Electrochemical experiments were recorded in acetonitrile solution that contained 0.1 M tetraethylammonium perchlorate (TEAP) as supporting electrolyte, under an argon atmosphere at room temperature (20°C). The working and auxiliary electrodes were platinum, the reference was a silver/silver chloride electrode modified for non-aqueous solvents and adjusted to 0.00 versus SCE. Cyclic voltammograms and controlled potential electrolysis were performed with a Wenking electrochemical system consisting of a voltage scan generator (model VSG-72) connected to a standard potentiostat (model ST-72), a voltage integrator (model EVI-80) and a Graphtec recorder (model WX-100).

Magnetic susceptibility measurements were made with a Bruker AC-200P spectrometer by the Evans method at 22°C [13].

2.2. Preparation of complexes

2.2.1. [(η⁶-MeC₆H₄Prⁱ)RuCl(η²-(EPPPh₂)₂CH₂-E,E')]BF₄ (E = S (1), Se (2))

A mixture of complex [((η⁶-MeC₆H₄Prⁱ)RuCl(μ-Cl))₂] (188 mg, 0.31 mmol), (EPPPh₂)₂CH₂ (0.68 mmol) and TIBF₄ (199 mg, 0.68 mmol) in acetone (40 ml) was stirred at room temperature for 12 h. The TiCl formed was filtered off through Kieselguhr, the solution evaporated to a small volume and the complex was isolated as yellow–red crystals by careful addition of n-hexane. **1**: yield 195 mg (79%). *Anal.* Found: C, 52.1; H, 4.4; S, 8.4. Calc. for C₃₅H₃₆BClF₄P₂RuS₂: C, 52.2; H, 4.5; S, 8.0%. IR (KBr): ν(P=S), 572 cm⁻¹. A_M = 120 cm² mol⁻¹ Ω⁻¹. **2**: yield 193 mg (70%). *Anal.* Found: C, 47.3; H, 4.4. Calc. for C₃₅H₃₆BClF₄P₂RuSe₂: C, 46.7; H, 4.0%. IR (KBr): ν(P=Se), 527 cm⁻¹. A_M = 118 cm² mol⁻¹ Ω⁻¹.

2.2.2. [(η⁶-MeC₆H₄Prⁱ)Ru(η³-(EPPPh₂)₂CH-C,E,E')]BF₄ (E = S (3), Se (4))

A mixture of complex **1** or **2** (0.11 mmol) and KOH (7.0 mg, 0.12 mmol) in methanol (20 ml) was boiled under reflux for 6 h. The solution was evaporated to dryness and the solid residue extracted with acetone. The complexes were precipitated by addition of n-hexane, as red–brown solids. **3**: yield 68 mg (80%). *Anal.* Found: C, 54.4; H, 4.3; S, 8.1. Calc. for C₃₅H₃₅BF₄P₂RuS₂: C, 54.6; H, 4.6; S, 8.3%. IR (KBr): ν(P=S), 572 cm⁻¹. A_M = 120 cm² mol⁻¹ Ω⁻¹. **4**: yield 67 mg (68%). *Anal.* Found: C, 48.6; H, 4.1. Calc. for C₃₅H₃₅BF₄P₂RuSe₂: C, 48.7; H, 4.1%. IR (KBr): ν(P=Se), 530 cm⁻¹. A_M = 119 cm² mol⁻¹ Ω⁻¹.

2.2.3. [(η⁶-MeC₆H₄Prⁱ)RuCl(η²-(SPPPh₂)₂CHMe-S,S')]BF₄ (5)

A mixture of complex [((η⁶-MeC₆H₄Prⁱ)RuCl(μ-Cl))₂] (200 mg, 0.33 mmol), (SPPPh₂)₂CHMe (330 mg, 0.71 mmol) and TIBF₄ (210 mg, 0.72 mmol) in acetone (20 ml) was stirred at room temperature for 4 h. The TiCl formed was filtered off through Kieselguhr, the solution evaporated to a small volume and the complex was isolated as red crystals by careful addition of n-hexane. Yield 214 mg (80%). *Anal.* Found: C, 51.2; H, 4.5; S, 7.7. Calc. for C₃₆H₃₈BClF₄P₂RuS₂: C, 52.7; H, 4.6; S, 7.8%. IR (KBr): ν(P=S), 594, 602 cm⁻¹. A_M = 143 cm² mol⁻¹ Ω⁻¹.

The similar hexafluorophosphate derivative was obtained using AgPF₆ instead of TIBF₄.

2.2.4. [(η⁶-MeC₆H₄Prⁱ)Ru(η³-(SPPPh₂)₂CMe-C,S,S')]PF₆ (6)

A mixture of complex **5** as hexafluorophosphate derivative (300 mg, 0.34 mmol) and TIPz [14] (93 mg, 0.34 mmol) in dichloromethane (20 ml) was stirred at room temperature for 4 h. The TiCl formed was filtered off through Kieselguhr, the solution evaporated to a small volume and the complex was isolated as red crystals by careful addition of diethyl ether. Yield 235 mg (82%). *Anal.* Found: C, 51.3; H, 4.2; S, 7.9. Calc. for C₃₆H₃₇F₆P₃RuS₂: C, 51.4; H, 4.4; S, 7.6%. IR (KBr): ν(P=S), 580 cm⁻¹. A_M = 144 cm² mol⁻¹ Ω⁻¹.

2.3. Crystal structure of 6

A red single crystal of 0.4 × 0.2 × 0.1 mm dimensions obtained by a slow diffusion of diethyl ether into a chloroform solution of complex **6** was selected for structure determination by X-ray diffraction. The summary of crystal data is given in Table 1. Intensity data were collected at 293 K on a Siemens P3/PC diffractometer using the θ/2θ scan technique and graphite monochromated Mo Kα radiation (λ = 0.71073 Å). A total of 4734 reflections with θ < 27° (0 ≤ h ≤ 19, 0 ≤ k ≤ 19, 0 ≤ l ≤ 20) was collected and merged to give 4158 independent reflections (R_{int} = 0.0089). The stability of the crystal during data collection was monitored by measuring two check reflections after every 98 measurements; their intensity variations were not larger than 2%.

Table 1

Crystal data for [(η⁶-MeC₆H₄Prⁱ)Ru(η³-(SPPPh₂)₂CMe-C,S,S')]PF₆

Empirical formula	C ₃₆ H ₃₇ F ₆ P ₃ S ₂ Ru
Formula weight (g mol ⁻¹)	841.76
Crystal system	tetragonal
Space group	P4 ₃
Unit cell dimensions	
a (Å)	15.120(2)
c (Å)	16.090(3)
Cell volume (Å ³)	3678.4(10)
Z	4
D _{calc} (Mg m ⁻³)	1.520
Absorption coefficient (mm ⁻¹)	0.726
F(000)	1712

The structure was solved by direct methods and refined by the full-matrix least-squares technique in the anisotropic approximation for all non-H atoms. All H atoms were placed in the geometrically calculated positions and refined in the isotropic approximation with the common temperature factor (which refined to the value of $0.16(1) \text{ \AA}^2$). The absolute structure was determined by means of the refinement of the Flack x parameter [15], which converged to the value of $0.02(8)$. Final discrepancy factors are $R1 = 0.0562$ (on F for 2418 reflections with $I > 2\sigma(I)$), $wR2 = 0.1923$ (on F^2 for all 4107 reflections used in the refinement of 434 parameters). All calculations were carried out on an IBM PC with the help of SHELXTL PLUS 5 (gamma version) program, written by Sheldrick (Göttingen, Germany). The same program was used for generation of the molecular drawing. The atomic coordinates and their equivalent isotropic temperature factors are listed in Table 2. The structure solution and refinement was severely complicated by the instability of the *p*-cymene group, which is manifested in high temperature factors of its atoms and inadequate bond distances (e.g. C(1)–C(2) 1.24(3), C(4)–C(5) 1.54(3), C(7)–C(9) 1.26(4)). This problem may be due either to the high thermal motion or, probably, some kind of statistical disorder in the crystal. Nevertheless, our sustained efforts to resolve the disorder and find any possible alternative positions for the *p*-cymene atoms did not yield any positive result. Moreover, the second low-temperature experiment, which was carried out at -80°C (unfortunately taken from a different specimen) did not yield any improvement either in respect to the temperature factors or the possible resolution of statistical disorder and, strangely enough, produced even worse general accuracy characteristics. We have also attempted to achieve disorder resolution performing the refinement on F for observed reflections (using the SHELXTL PLUS Version 4 programs), rather than on F^2 for all reflections. However, in accordance with our general previous experience with unstable refinements, the F^2 refinement proved to produce better results. In spite of the above problems with the *p*-cymene moiety the overall chemical connectivity as well as the geometry of the rest of the structure do not raise any doubts and may be discussed, provided the proper care is exercised. See also Section 4.

3. Results and discussion

The binuclear complex $\{[(\eta^6\text{-MeC}_6\text{H}_4\text{Pr}^i)\text{RuCl}(\mu\text{-Cl})_2]\}$ reacts in acetone with the ligands $(\text{EPPH}_2)_2\text{CH}_2$ (E = S, Se) in the presence of thallium tetrafluoroborate yielding the cationic compounds $\{[(\eta^6\text{-MeC}_6\text{H}_4\text{Pr}^i)\text{RuCl}\{\eta^2\text{-}(\text{EPPH}_2)_2\text{CH}_2\text{-E,E'}\}]\text{BF}_4$ (E = S (1), Se (2)). These complexes react with potassium hydroxide in refluxing methanol by deprotonation of the methylene group of the coordinated ligand, yielding new cationic complexes of formula $\{[(\eta^6\text{-MeC}_6\text{H}_4\text{Pr}^i)\text{Ru}\{\eta^3\text{-}(\text{EPPH}_2)_2\text{CH-C,E,E'}\}]\text{BF}_4$ (E = S (3), Se (4)).

Table 2

Atomic coordinates ($\times 10^4$) and equivalent isotropic temperature factor ($\text{\AA}^2 \times 10^3$) for complex **6** (with e.s.d.s in parentheses)

	<i>x</i>	<i>y</i>	<i>z</i>	U_{eq}^a
Ru(1)	6956(1)	8893(1)	1253(1)	70(1)
S(1)	7609(4)	9873(3)	2298(3)	128(2)
S(2)	7991(2)	7819(3)	1781(2)	102(1)
P(1)	6555(2)	9478(2)	2943(2)	73(1)
P(2)	6984(2)	7539(2)	2528(2)	64(1)
P(3)	3899(2)	7335(2)	5087(2)	85(1)
F(1)	4428(9)	7368(15)	4241(7)	219(8)
F(2)	3360(11)	7328(25)	5899(10)	326(16)
F(3)	4201(13)	8234(8)	5403(17)	239(9)
F(4)	3627(11)	6419(8)	4870(14)	208(7)
F(5)	3038(10)	7641(12)	4731(10)	207(7)
F(6)	4781(8)	6840(9)	5501(9)	165(4)
C(1)	7511(12)	9538(14)	115(12)	132(7)
C(2)	7535(17)	8731(19)	-14(10)	136(7)
C(3)	6776(23)	8243(12)	49(10)	132(8)
C(4)	5897(16)	8644(22)	339(12)	176(13)
C(5)	5988(10)	9646(12)	513(9)	101(4)
C(6)	6785(18)	10003(10)	400(11)	105(4)
C(7)	8439(18)	10035(29)	58(23)	301(29)
C(8)	8430(18)	10516(23)	-810(18)	283(24)
C(9)	9138(18)	9824(19)	440(30)	251(22)
C(10)	4907(22)	8336(26)	398(17)	426(46)
C(11)	6267(6)	8465(6)	2418(6)	58(2)
C(12)	5283(7)	8295(7)	2365(7)	71(3)
C(13)	5619(12)	10231(7)	2880(7)	94(4)
C(14)	4836(13)	10049(12)	3274(8)	118(6)
C(15)	4168(16)	10671(17)	3210(9)	158(10)
C(16)	4228(29)	11403(23)	2811(19)	234(24)
C(17)	5092(35)	11586(13)	2382(16)	256(27)
C(18)	5741(16)	11023(8)	2424(8)	136(8)
C(19)	6810(10)	9416(7)	4043(7)	84(3)
C(20)	6195(13)	9077(16)	4613(8)	140(7)
C(21)	6420(15)	9028(15)	5471(11)	139(7)
C(22)	7198(16)	9250(13)	5714(10)	124(6)
C(23)	7823(16)	9532(15)	5191(14)	147(8)
C(24)	7605(12)	9629(10)	4305(10)	108(5)
C(25)	6385(9)	6562(7)	2188(7)	78(3)
C(26)	5624(13)	6263(8)	2568(8)	110(5)
C(27)	5213(18)	5497(10)	2331(10)	136(7)
C(28)	5487(19)	5039(13)	1705(16)	149(8)
C(29)	6240(16)	5282(14)	1295(16)	157(9)
C(30)	6717(11)	6117(11)	1494(11)	118(5)
C(31)	7376(7)	7294(6)	3576(6)	68(3)
C(32)	6816(9)	7043(15)	4284(9)	127(6)
C(33)	7129(13)	6874(13)	4977(9)	116(5)
C(34)	7962(13)	69301(9)	5128(9)	101(4)
C(35)	8546(14)	7203(16)	4546(14)	145(7)
C(36)	8233(9)	7344(10)	3755(10)	104(4)

^a U_{eq} is defined as one third of the trace of the orthogonalised U_{ij} tensor.

The ^1H NMR spectra exhibit the expected resonances of the *p*-cymene ligand. For complexes **1** and **2**, the spectra show two doublets of doublets in the range δ 4.56–5.54 ppm corresponding to the non-equivalent methylene protons H_a and H_b , where H_a is the proton *endo* to the chlorine atom [7,8]. Complexes **3** and **4** show only one resonance at δ 3.29 (s, br) and 3.68 (t, $^2J_{\text{PH}} = 1.7$ Hz) ppm, respectively, confirming that the methylene group in the starting complexes undergoes

deprotonation. In a similar fashion to the related rhodium, iridium and ruthenium derivatives [6–9], their $^{13}\text{C}\{^1\text{H}\}$ NMR spectra show the expected strong shielding increase of the methanide carbon, which appears as a triplet signal at δ –30.18 and –31.71 ppm, respectively. The $^{31}\text{P}\{^1\text{H}\}$ NMR spectra exhibit a singlet resonance for the equivalent P(E) group and compounds **2** and **4** show the corresponding P–Se coupling. Relevant NMR chemical shifts and coupling constants are listed in Table 3.

Similarly, the ligand $(\text{SPPPh}_2)_2\text{CHMe}$ reacts with the binuclear complex $[(\eta^6\text{-MeC}_6\text{H}_4\text{Pr}^t)\text{RuCl}(\mu\text{-Cl})_2]$ in acetone solution in the presence of TlBF_4 or AgPF_6 to give the cationic complex $[(\eta^6\text{-MeC}_6\text{H}_4\text{Pr}^t)\text{RuCl}\{\eta^3\text{-}(\text{SPPPh}_2)_2\text{CHMe-S,S}'\}]^+$ (**5**). The ^1H NMR spectrum shows a multiplet resonance at δ 4.86 ppm for the methylene proton and a doublet of triplets at δ 1.58 ppm with $^3J_{\text{PH}} = 17.2$ Hz and $^3J_{\text{HH}} = 7.4$ Hz, corresponding to the methyl group of the chalcogenide ligand and the $^{13}\text{C}\{^1\text{H}\}$ NMR spectrum shows a triplet resonance for the methylene carbon at δ 35.49 ppm ($^1J_{\text{PC}} = 42.5$ Hz). When complex **5** was treated with thallium pyrazolate in dichloromethane solution, the chloride ligand was eliminated as TlCl and the coordinated ligand deprotonated by the pyrazolate group yielding the new cationic compound $[(\eta^6\text{-MeC}_6\text{H}_4\text{Pr}^t)\text{Ru}\{\eta^3\text{-}(\text{SPPPh}_2)_2\text{CMe-C,S,S}'\}]^+$ (**6**), in which the ligand is acting as a tridentate ligand with a C,S,S'-donor set. Their ^1H NMR spectra exhibit only a triplet resonance for the methyl group at δ 2.15 ppm with $^3J_{\text{PH}} = 18.6$ Hz, and the $^{13}\text{C}\{^1\text{H}\}$ NMR spectrum shows a triplet resonance for the methanide carbon at δ –19.8 ppm ($^1J_{\text{PC}} = 36.5$ Hz).

All cationic compounds were isolated as stable microcrystalline solids and behave as 1:1 electrolytes in acetone solution. Their IR spectra in KBr pellets show the presence of uncoordinated BF_4^- (~ 1100 and 520 cm^{-1}) or PF_6^- (~ 840 and 560 cm^{-1}) anion together with the absorptions bands corresponding to the P=S or P=Se groups, shifted to lower frequencies ($\nu(\text{PS})$, 572–602 cm^{-1} ; $\nu(\text{PSe})$, 527–530 cm^{-1}) relative to the free ligands ($\nu(\text{PS})$, 628 cm^{-1} ; $\nu(\text{PSe})$, 531 cm^{-1}) [16,17].

The structure of complex **6**, as the hexafluorophosphate derivative, was established by X-ray diffraction. Fig. 1 shows the structure of both the cation and anion of complex **6** with the atom numbering scheme. In the cation the ruthenium atom has a distorted octahedral coordination with the *p*-cymene ligand occupying three octahedral sites and the bis(diphenylphosphine)methyl methanide disulfide ligand bonded to the ruthenium atom via two sulfur atoms and the methanide carbon atom. Selected bond lengths and angles are listed in Table 4.

The Ru–C(ring) distances span the range 2.183–2.237 Å and are comparable to those found for other related complexes [18–20]. The Ru–S (2.421(4) and 2.449(4) Å) and Ru–C(11) (2.239(10) Å) distances are similar to those found in the related compound $[(\eta^6\text{-C}_6\text{Me}_6)\text{Ru}\{\eta^3\text{-}(\text{SPPPh}_2)_2\text{CH-C,S,S}'\}]\text{ClO}_4$ (Ru–S 2.443(1) and Ru–C 2.238(4) Å) [8].

The P–S (1.982(4) and 1.993(5) Å) and P–C(11) (1.803(9) and 1.781(10) Å) distances of the coordinated anionic tridentate ligand are in agreement with those found in $[(\eta^6\text{-C}_6\text{Me}_6)\text{Ru}\{\eta^3\text{-}(\text{SPPPh}_2)_2\text{CH-C,S,S}'\}]\text{ClO}_4$ (P–S

Table 3
NMR chemical shifts (δ ppm) and coupling constants (Hz) of ruthenium(II) complexes ^a

Complex	^1H				$^{31}\text{P}\{^1\text{H}\}$
	Arene				
	Pr ^t	Me	H	CH ₂ (CH), CHMe(CMe)	
1	1.41 [d, Me, $^3J(\text{HH}) = 6.9$] 3.05 (m, CH)	2.33 (s)	5.69 (d), 5.81 (d) $^3J(\text{HH}) = 6.1$	5.00 (dt, H _a), 5.54 (dt, H _b) $^3J(\text{PH}_a) = 12.8$, $^3J(\text{PH}_b) = 15.6$ $^3J(\text{HH}) = 14.5$	37.81 (s)
2	1.20 [d, Me, $^3J(\text{HH}) = 6.9$] 2.84 (m, CH)	2.11 (s)	5.27 (d), 5.39 (d) $^3J(\text{HH}) = 6.1$	4.56 (dt, H _a), 5.00 (dt, H _b) $^3J(\text{PH}_a) = 14.8$, $^3J(\text{PH}_b) = 12.3$ $^3J(\text{HH}) = 14.8$	19.21 (s) $^1J(\text{PSe}) = 635.5$ $^2J(\text{PSe}) = 5.23$
3^b	1.15 [d, Me, $^3J(\text{HH}) = 6.9$] 2.47 (m, CH)	1.43 (s)	4.70 (d), 5.25 (d) $^3J(\text{HH}) = 6.0$	3.29 (s, br)	55.10 (s)
4^c	1.11 [d, Me, $^3J(\text{HH}) = 6.9$] 2.52 (m, CH)	1.43 (s)	4.62 (d), 5.19 (d) $^3J(\text{HH}) = 5.9$	3.68 [t, $^2J(\text{PH}) = 1.70$]	41.20 (s) $^1J(\text{PSe}) = 512.7$
5^d	1.16 [d, Me, $^3J(\text{HH}) = 6.9$] 2.65 (m, CH)	2.08 (s)	5.30 (d), 5.41 (d) $^3J(\text{HH}) = 6.9$	1.58 [dt, Me, $^3J(\text{PH}) = 17.2$, $^3J(\text{HH}) = 7.4$], 4.86 (m, H)	43.79 (s)
6^e	1.32 [d, Me, $^3J(\text{HH}) = 6.9$] 2.90 (m, CH)	1.51 (s)	4.94 (d), 5.34 (d) $^3J(\text{HH}) = 6.0$	2.15 [t, Me, $^3J(\text{PH}) = 18.6$]	65.47 (s)

^a Measured in CDCl_3 at room temperature. Chemical shifts relative to Me_4Si and H_3PO_4 (85%) as standards. All complexes show multiplets in the region δ 7.4–8.0 ppm corresponding to the phenyl groups of the chalcogenide ligands.

^b $^{13}\text{C}\{^1\text{H}\}$ NMR (CDCl_3): δ –30.18 ppm [t, CH, $^1J(\text{PC}) = 51.3$ Hz].

^c $^{13}\text{C}\{^1\text{H}\}$ NMR (CDCl_3): δ –31.71 ppm [t, CH, $^1J(\text{PC}) = 39.3$ Hz].

^d $^{13}\text{C}\{^1\text{H}\}$ NMR (CDCl_3): δ 35.49 [t, CHMe, $^1J(\text{PC}) = 42.5$ Hz], 15.67 (s, CHMe) ppm.

^e $^{13}\text{C}\{^1\text{H}\}$ NMR (CDCl_3): δ –19.8 [t, CMe, $^1J(\text{PC}) = 36.5$ Hz], 23.53 (s, CMe) ppm.

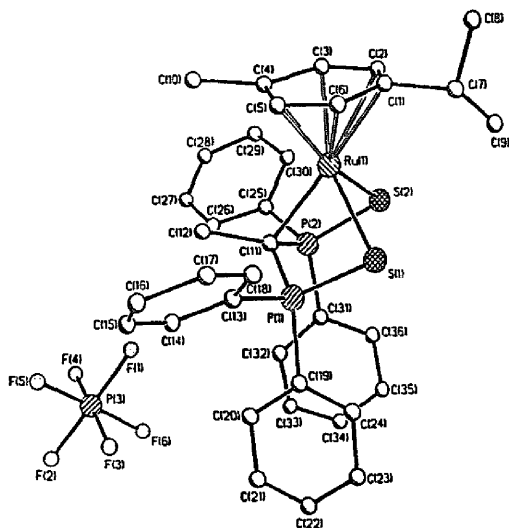


Fig. 1. View of the structure of the complex $[\{\eta^3\text{-MeC}_2\text{H}_4\text{P}^+\text{-Ru}\{\eta^3\text{-(SPPPh}_2\text{)}_2\text{CMe-C,S,S}'\}\text{PF}_6]$, showing the atom numbering. Hydrogen atoms have been omitted for clarity.

Table 4

Selected bond distances (Å) and bonds angles (°) of complex 6 (with e.s.d.s in parentheses)

Ru–S(1)	2.449(4)	Ru–C(1)	2.237(14)
Ru–S(2)	2.421(4)	Ru–C(2)	2.230(2)
Ru–C(11)	2.239(10)	Ru–C(3)	2.190(2)
P(1)–S(1)	1.993(5)	Ru–C(4)	2.206(14)
P(2)–S(2)	1.982(4)	Ru–C(5)	2.200(2)
P(1)–C(11)	1.803(9)	Ru–C(6)	2.183(13)
P(2)–C(11)	1.781(10)		
S(1)–Ru–S(2)	84.7(2)	C(11)–P(1)–S(1)	101.7(4)
S(1)–Ru–C(11)	77.7(2)	C(11)–P(1)–C(19)	117.7(5)
S(2)–Ru–C(11)	79.1(3)	C(11)–P(1)–C(13)	108.5(5)
Ru–S(1)–P(1)	81.6(2)	C(13)–P(1)–C(19)	104.6(6)
Ru–S(2)–P(2)	81.7(13)	C(13)–P(1)–S(1)	114.0(5)
Ru–C(11)–P(1)	92.0(4)	C(19)–P(1)–S(1)	110.7(5)
Ru–C(11)–P(2)	91.6(4)	C(11)–P(2)–S(2)	104.2(3)
P(1)–C(11)–P(2)	118.3(5)	C(11)–P(2)–C(25)	107.8(5)
C(12)–C(11)–Ru	117.4(7)	C(11)–P(2)–C(31)	116.7(5)
C(12)–C(11)–P(1)	114.1(7)	C(25)–P(2)–C(31)	105.9(5)
C(12)–C(11)–P(2)	118.1(7)	C(31)–P(2)–S(2)	110.7(4)
		C(25)–P(2)–S(2)	111.6(4)

2.003(1) and P–C 1.775(2) Å [8], and the P–S and P–C distances are slightly shorter and slightly longer, respectively, as compared to those found in complexes containing the anionic ligand coordinated in their bidentate S,S'-donor form, such as $[\text{Rh}(\text{cod})\{\eta^2(\text{SPPPh}_2)_2\text{CH-S,S}'\}]$ (P–S(av.) 2.036(4) and P–C 1.705(11) Å) and $[\text{Ir}(\text{cod})\{\eta^2(\text{SPPPh}_2)_2\text{CH-S,S}'\}]$ (P–S(av.) 2.039(3) and P–C 1.711(6) Å) [3].

The methanide carbon atom C(11) has a severely distorted tetrahedral environment, which is characterised by considerable decrease of the two angles formed by the Ru–C(11) and Ru–P bonds (Ru(1)–C(11)–P(1) 92.0(4) and Ru(1)–C(11)–P(2) 91.6(4)°) and corresponding increase of the remaining four angles in the tetrahedron

3.1. Electrochemical data

The cyclic voltammograms of ligands $(\text{SPPPh}_2)_2\text{CH}_2$ and $(\text{SPPPh}_2)_2\text{CHMe}$ in acetonitrile exhibit a broad peak at 1.20–1.24 V versus SCE corresponding to an irreversible oxidation and two small reduction peaks at –0.18 and –1.41 V versus SCE coupled to it. The electrochemical data of the cationic compounds 1, 3, 5 and 6 in acetonitrile solution are summarised in Table 5.

The cationic complexes containing neutral disulfide ligands, 1 and 5, present a similar electrochemical behaviour. Fig. 2A shows the cyclic voltammogram of a 5.0 mM solution of complex 5. For an initial negative scan four highly irreversible reductions are observed. Controlled potential electrolysis at –1.10 V versus SCE indicates that one equivalent of charge is being transferred in this process. The resulting red-brown solution exhibits two irreversible reduction peaks at –1.34 and –1.96 V versus SCE (Fig. 2B). The cyclic voltammogram of complex 6 shows a similar irreversible reduction pattern (Fig. 2D). Controlled potential electrolysis at –1.50 V versus SCE results in the consumption of one Faraday mol^{-1} in the second reduction process and the dark brown solution formed does not undergo reductions in the potential range used, –2.00 to +1.80 (Fig. 2B, dotted line).

Complex 3 exhibits three reduction peaks (Fig. 2C). However if the scan is reversed after the first peak one well-defined redox couple is observed. The peak separation ($\Delta E_p = 0.24$ V) and I_{pa}/I_{pc} ratio (0.63) indicates that this quasi-reversible process has coupled to a chemical reaction (EC mechanism) [21]. Controlled potential electrolysis after the first peak (–1.50 V versus SCE) indicates that one equivalent of charge per mole of ruthenium is transferred. The dark brown compound has been found to be unstable in the bulk electrolysis time scale and its cyclic voltammogram does not show the oxidation peak at –1.10 V versus SCE.

Fig. 2D shows the cyclic voltammogram of a 5.0 mM solution of complex 6. This compound also exhibits a quasi-reversible redox couple at –1.34/–0.68 V versus SCE ($\Delta E_p = 0.66$, $I_{pa}/I_{pc} = 0.35$) and one irreversible charge transfer process at –1.96 V. Controlled potential electrolysis at –1.50 V indicates that one equivalent of charge is transferred in this process.

Table 5

Electrochemical parameters of complexes 1, 3, 5 and 6^a

Complex	E_{peak} (V)	
	Reductions	Oxidations
1	–1.12, –1.35, –1.67, –1.85	1.20, 1.45
3	–1.34, –1.64, –1.86, 0.66	–1.10, 1.26
5	–1.08, –1.21, –1.34, –1.84	1.22, 1.48
6	–1.34, –1.96, 1.08, 0.66	–0.68, 1.24

^a Potential values obtained on 0.1 M TEAP/MeCN solutions of the complexes and referred to the saturated calomel electrode (SCE). The scan rate was 200 mV s^{-1} .

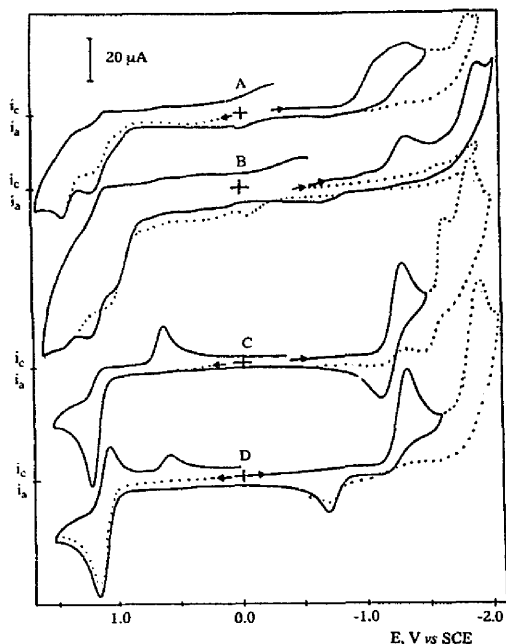
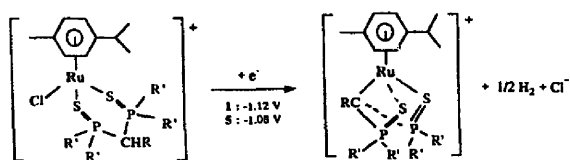


Fig. 2. Cyclic voltammograms of 5 mM solutions of complexes in acetonitrile using 0.1 M tetraethylammonium perchlorate (TEAP) as supporting electrolyte. A, 5; B, electrolytical solution of 5; C, 3; D, 6. The scan rate is 0.2 V s^{-1} in all cases. The working electrode is a platinum disc.

In order to identify the species associated with each individual redox process, the electrolytical solutions were evaporated to dryness, the solid residues dissolved in deuterated chloroform and the solutions analysed by ^1H and $^{31}\text{P}\{^1\text{H}\}$ NMR spectroscopy. These spectra show the resonances corresponding to deprotonated complexes **3** and **6**, which are formed in the first reduction of complexes **1** ($E_p = -1.12 \text{ V}$) and **5** ($E_p = -1.08 \text{ V}$), respectively (Scheme 1). Later, the deuterated solvent was changed to acetonitrile and the rescan cyclic voltammograms show that the redox properties did not change.

On the other hand, cyclic voltammograms of these electrolytical solutions show the presence of free chloride ions generated during the electrolysis (oxidation at 1.06 V versus SCE, Fig. 2B). Cyclic voltammograms of complexes **3** or **6** in the presence of LiCl are identical to the cyclic voltammograms of reduced complexes **1** or **5**.

Complexes **1** and **5** are unstable in acetonitrile and dichloromethane solutions. The presence of free ligand was detected by NMR spectra and cyclic voltammograms (oxidation at 1.20 – 1.24 V versus SCE) before the electrolysis



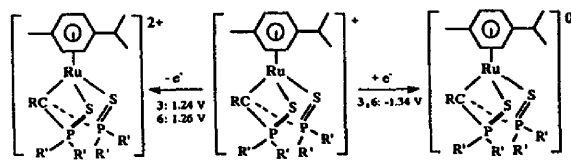
Scheme 1. (R = H (**1**), Me (**5**); R' = Ph).

was carried out. The second cathodic processes of these complexes is identical to the first reduction of complexes **3** and **6**, and should correspond to the one-electron reduction of the complexes to a ruthenium(I) species which rapidly decomposes in solution. NMR spectra indicate the presence of the initial complex of Ru(II), free ligand and other uncharacterised species. These products do not show magnetic susceptibility and EPR response. The presence of chloride ions possibly affects the stability of the Ru(I) species and changes the reversibility of the redox couple Ru(II)–Ru(I) as shown by the disappearance of the peak that corresponds to the oxidation process. The second electrolysis of complexes **1** or **5** gives a black solid, probably due to formation of an Ru(0) species, which was adsorbed at the platinum mesh. These results are in agreement with those reported for related Ru(II) complexes which are directly reduced to Ru(0), without evidence of the stabilisation of Ru(I) intermediates [22].

When scanning toward positive potentials, the cyclic voltammograms of compounds **1** and **5** show anodic peaks. The presence of free ligand is detected for the small oxidation at 1.20 – 1.24 V versus SCE. The controlled potential electrolysis at $+1.60 \text{ V}$ versus SCE ($E_{\text{peak}} = 1.48 \text{ V}$, Fig. 2A) indicates that one equivalent of charge is being transferred in this process. The cyclic voltammograms of these solutions show several peaks which would be indicative of the instability of the complexes. On the other hand, the cyclic voltammograms of compounds **3** and **6** show only one anodic peak at 1.26 and 1.24 V versus SCE, respectively (Fig. 2C and D). Controlled potential electrolysis at 1.50 V versus SCE shows the transfer of one equivalent of charge yielding a green solution of a ruthenium(III) species. The compound produced in this process is stable and their cyclic voltammograms show a quasi-reversible redox couple with an anodic peak at $+0.66 \text{ V}$ and a cathodic peak at $+0.60 \text{ V}$ versus SCE (for compound **3**), that would correspond to the oxidation of ruthenium(III) to ruthenium(IV) and the corresponding reduction.

These results indicate that the principal electrochemical reactions for deprotonated complexes proceed according to Scheme 2.

In contrast with complexes **1** and **5**, the acetonitrile solutions of complexes **3** and **6** do not show the presence of the free ligand, indicating that deprotonation of the ligands and coordination in their tridentate form stabilise the ruthenium(II) compounds. Complexes **3** and **6** have similar stabilities since the reduction and oxidation of the metallic ion occurs at similar potentials (Ru(II) to Ru(I) at -1.34 V and Ru(II) to Ru(III) at 1.26 and 1.24 V for complexes **3** and **6**, respectively). However, the reversibility and current ratio are



Scheme 2. (R = H (**3**), Me (**6**); R' = Ph).

very different (Fig. 2C and D), indicating different stabilities of the Ru(I) and Ru(III) species.

4. Supplementary material

Lists of observed and calculated structure factors (9 pages), anisotropic thermal parameters, H atom coordinates, full list of bond lengths and angles, and least-squares planes are available from the authors on request.

Acknowledgements

The authors are indebted to Dr A.I. Yanovsky and F.M. Dolgushin from the X-ray Structural Centre (XRSC) of the General and Technical Chemistry Division of the Russian Academy of Sciences for carrying out the X-ray structure solution. Financial support by the Fondo Nacional de Ciencia y Tecnología (FONDECYT, Grant No. 460/93) is gratefully acknowledged.

References

- [1] D.E. Berry, J. Browning, K.R. Dixon, R.W. Hiltz and A. Pidcock, *Inorg. Chem.*, **31** (1992) 1479.
- [2] R. Contreras, M. Valderrama and S. Yañez, *Transition Met. Chem.*, **18** (1993) 73.
- [3] J. Browning, G.W. Bushnell, K.R. Dixon and R.W. Hiltz, *J. Organomet. Chem.*, **434** (1992) 241.
- [4] A. Laguna and M. Laguna, *J. Organomet. Chem.*, **394** (1990) 743.
- [5] A. Laguna, M. Laguna, A. Rojo and M.N. Fraile, *J. Organomet. Chem.*, **315** (1986) 269.
- [6] M. Valderrama, R. Contreras, M. Bascuñán and D. Boys, *Polyhedron*, **13** (1994) 1101.
- [7] M. Valderrama and R. Contreras, *Bol. Soc. Chil. Quím.*, **40** (1995) 111.
- [8] M. Valderrama, R. Contreras, M. Bascuñán, S. Alegría and D. Boys, *Polyhedron*, **14** (1995) 2239.
- [9] M. Valderrama and R. Contreras, *J. Organomet. Chem.*, **513** (1996) 7.
- [10] S.O. Grim and F.D. Walton, *Inorg. Chem.*, **19** (1980) 1982.
- [11] S.O. Grim and J.D. Mitchell, *Inorg. Chem.*, **16** (1977) 1762.
- [12] M.A. Bennett and A.K. Smith, *J. Chem. Soc., Dalton Trans.*, (1974) 233.
- [13] D.F. Evans, *J. Chem. Soc.*, (1959) 2003.
- [14] M. Scotti, M. Valderrama, R. Moreno, R. López and D. Boys, *Inorg. Chim. Acta*, **216** (1994) 67.
- [15] H.D. Flack, *Acta Crystallogr., Sect. A*, **39** (1983) 876.
- [16] E.W. Ainscough, H.A. Bergen, A.M. Brodie and K.A. Brown, *J. Chem. Soc., Dalton Trans.*, (1976) 1649.
- [17] S.W. Carr and R. Colton, *Aust. J. Chem.*, **34** (1981) 35.
- [18] J. Browning, G.W. Bushnell, K.R. Dixon and R. Hiltz, *J. Organomet. Chem.*, **452** (1993) 205.
- [19] L.A. Oro, D. Carmona, M.P. García, F.J. Lahoz, J. Reyes, C. Foces-Foces and F.H. Cano, *J. Organomet. Chem.*, **296** (1985) C43.
- [20] L.A. Oro, M.P. García, D. Carmona, C. Foces-Foces and F.H. Cano, *Inorg. Chim. Acta*, **96** (1985) L21.
- [21] J. Heinze, *Angew. Chem., Int. Ed. Engl.*, **23** (1984) 831.
- [22] P. Lahuerta, J. Latorre, M. Sanau, F.A. Cotton and W. Schwotzer, *Polyhedron*, **7** (1988) 1311.